1990年度 大韓醫用生體工學 秋季 學術大會 論文集 90/11

MR Gradient Echo 영상술에서 자화율에 의한 에러의 감소에 관한 연구

노용만, 조장희
한국과학기술원, 전기및 전자공학과

Reduction of Susceptibility Artifact in MR Gradient Echo Imaging

Y.M. Ro and Z.H. Cho
Department of Electrical Science, Korea Advanced Institute of Science,
P.O. Box 150, Chongyangni, Seoul, Korea

Abstract

A new technique for reducing the susceptibility artifact in gradient echo imaging which uses a tailored RF pulse is proposed. It is applied to the case of imaging where artifacts and distortions arise due to the high local magnetic field inhomogeneity i. e., the susceptibility. The signal loss and void phenomena due to susceptibility in a voxel are studied and a correction method using a tailored RF pulse is proposed. Applications of this method in imaging are given and experimental results obtained using an human volunteer with a 2.0 T KAIS NMR system are presented.

I. Introduction

Since the introduction of the gradient echo technique, it has become possible to achieve many fast MR imagings such as the SSFP (1,2,3,4), FLASH (5,6) and GRASS (7,8). These techniques, however, have been difficult to use in clinical situations due to the severe inhomogeneity artifacts arising from the gradient refocusing inherent in method. Consequently usage of the various gradient echo techniques has been limited. Although whole-body magnets which have superior field homogeneity are available today, the gradient echo techniques still suffer from the local field inhomogeneity, i.e., inhomogeneity due to susceptibility. This local field inhomogeneity often leads to severe artifacts in images (9,10,11). While inhomogeneities due to the chemical shifts or static fields can be corrected (12,13), correction of susceptibility effects arising from such problems as the air-tissue interface around the nasal cavity in human head image has been particularly difficult (10). This is mainly due to the fact that gradient echo imaging dephases the spins within a selected slice because of local field inhomogeneity induced by the susceptibility. In other words, the precession frequencies of the spins within a voxel become different from one another according to the local field inhomogeneity. Consequently the magnetization of the dephased spins in a voxel mutually cancel so that the signal from the voxel is reduced. Correction of highly localized field inhomogeneities due to the susceptibility has been especially difficult because of relatively sudden changes or a highly localized nature. The susceptibility artifacts are especially pronounced when the thickness of the slice selection is large since larger phase spreads along the direction of the slice tend to cancel out the average signal received.

Recently, several papers have been published aiming to reduce susceptibility artifacts in MR imaging (14,15,16). One of the proposed methods is reduction of the voxel size, suggested by I. R. Young et al. (14). Here susceptibility artifacts are reduced by limiting the region so that the field inhomogeneity is proportionally reduced. This method, however, has limitations such as a poor signal-to-noise ratio thereby producing an unnecessarily noisy image. Another method proposed by J. Frahm et al. (15) uses the gradient compensation method where the biological susceptibility can be recovered locally by using a slightly modified slice selection gradient and increased imaging time.

In what follows we will describe the characteristics of the inhomogeneity due to the susceptibility, resulting phase dispersions along the direction of the slice, and a possible correction scheme which restores the signal strength.

II. Theory and Methods

Signal Loss due to Susceptibility Effect in a Voxel

As is known, the selected slice thickness in most MR imaging techniques tends to be larger than the resolution in the transverse plane. Therefore, this thickness in gradient echo techniques tends to disperse the phase during the echo time and results in discrepancies of the spins within the voxel. This

situation is illustrated in Fig. 1. Here we have assumed that the signal loss due to a voxel's susceptibility is mainly due to the finite thickness of the image plane, and other factors are assumed negligible. Let us assume that if the RF pulse is excited with a slice selection gradient, spins will flip on the selected transverse plane, and are expected to be dephased due to field inhomogeneity as shown in Fig. 1 (a) and (b). In an ideal case with no field inhomogeneity, and provided a perfect linear gradient and rectangular selection RF pulse are applied, well-refocused spins will be observed at the time of the echo position, and consequently a large signal will result due to the increased vector sum of the spins. If field inhomogeneity due to the susceptibility is introduced, i.e., a strong localized gradient existing within a voxel as shown in Fig. 2 (b), the resulting phase distribution will be incoherent as shown in Fig. 1 (b), and the resulting vector sum will produce a weak signal. Now let us consider that, normally, the total signal obtainable in NMR is given by:

$$S = \sqrt{R^2 + I^2} \qquad [1]$$

where S represents the detected signal, and R and I are the sum of real and imaginary components of magnetization in a voxel. Because of the fact that phase dispersion is due to field inhomogeneity, both the real and imaginary components represent the sum of the transverse magnetization components along the slice thickness. In other words,

$$R = \int_{voxel} M \cos\theta(v)\, dv = \iiint_{x\,y\,z} M \cos\theta(x,y,z)\, dxdydz \qquad [2]$$

and

$$I = \int_{voxel} M \sin\theta(v)\, dv = \iiint_{x\,y\,z} M \sin\theta(x,y,z)\, dxdydz \qquad [3]$$

where M is the magnetization and $\theta(x,y,z)$ is the phase distribution of spins in three dimensions. Let us assume that the phase distribution of the spins varies only in the direction of slice selection (z direction) and the phase distributions are uniform in the other directions (x and y directions or within the transverse plane). To simplify the analysis, we have also assumed that resolutions in the transverse plane are normalized and the slice is selected from $-Z_o/2$ to $Z_o/2$ in z direction so that the slice thickness equals Z_o. R and I, then, can be rewritten as

$$R = \int_{-\frac{z_o}{2}}^{\frac{z_o}{2}} M \cos\theta(z)\, dz, \qquad [4]$$

and

$$I = \int_{-\frac{z_o}{2}}^{\frac{z_o}{2}} M \sin\theta(z)\, dz, \qquad [5]$$

where $\theta(z)$ is the phase along the z direction or slice thickness direction. One can also assume that the value of $\theta(z)$ is linearly proportional to the position along the slice thickness as implied in Fig. 2 (b), i.e., $\theta(z) = P_{sus}z$. This assumption is valid since the field inhomogeneity due to susceptibility is usually highly localized, and therefore, quite steep gradients are common as shown in Fig. 2 (b). One can define, in conjunction with the susceptibility, the phase gradient P_{sus} as:

$$P_{sus} = \gamma\, TE\, G_{sus}, \qquad [6]$$

where γ is the gyromagnetic ratio, and TE is the echo time, and G_{sus} is the field gradient created by the susceptibility effect, respectively. The signal S in Eq. [1], then, can be rewritten as:

$$S = \sqrt{\left\{\int_{-\frac{z_o}{2}}^{\frac{z_o}{2}} M\cos(P_{sus}z)\, dz\right\}^2 + \left\{\int_{-\frac{z_o}{2}}^{\frac{z_o}{2}} M\sin(P_{sus}z)\, dz\right\}^2} \qquad [7]$$

Note here that the second bracket corresponding to the imaginary part will become zero in normal cases since $M\sin(P_{sus}z)$ is the odd function, and the first bracket leads to the well-known sinc(·) function. Eq. [7], therefore, becomes:

$$S = M z_o \left| \mathrm{sinc}\left(\frac{P_{sus}}{2} z_o\right)\right| \qquad [8]$$

Implications of Eq. [8] will be discussed in the following.

Compensation of The Susceptibility Induced Signal Loss

Let us now consider two different field inhomogeneities within a given voxel, namely, a case where one field is constant or homogeneous like voxel "A" and the other has a linear gradient field with phase distribution $\theta(z) = P_{sus}z$ as shown in Fig. 2 (a) and (b). The latter could be a case where the local susceptibility induces a field like voxel "B".

As described below, such a case of signal loss due to the susceptibility or the phase gradient created by the susceptibility can be minimized by using a suitably tailored RF pulse. As is known, the RF pulse in conventional imaging generally has a constant phase distribution, i.e., the spin phases within the selected slice (voxel) are constant in the direction of the slice selection. If the RF pulse is suitably tailored such that it has a quadratic phase ($\theta_p(z) = az^2$)

distribution along the direction of the slice selection, as shown in Fig. 2 (c), it can compensate for much of the phase gradient due to the susceptibility. In other words, by superimposing the phase-compensating RF pulse on the field inhomogeneity (created because of the susceptibility), it is possible to create a distribution which has minimal total phase variations. An example of the quadratic phase and linear field inhomogeneity can be as:

$$\theta(z) = \theta_p(z) + P_{sus}\, z = a\, z^2 + P_{sus}\, z \qquad [9]$$

where "a" is a coefficient chosen as the design parameter of the RF pulse. Fig. 2 (c) shows a sample case where a quadratic phase RF pulse is applied to voxel "A" where the field is homogeneous. Fig. 2 (d) represents the phase distribution of the spins when the same RF pulse is applied to voxel "B" where inhomogeneity exists as a susceptibility-caused linear field gradient. Where the quadratic phase generated by the RF pulse is superimposed on a local inhomogeneity (linear phase $P_{sus}z$), the acquired real and imaginary parts of signal can be written as:

$$R = \int_{-\frac{z_0}{2}}^{\frac{z_0}{2}} M \cos(az^2 + P_{sus}z)\, dz \qquad [10]$$

and

$$I = \int_{-\frac{z_0}{2}}^{\frac{z_0}{2}} M \sin(az^2 + P_{sus}z)\, dz\,. \qquad [11]$$

Then Eq. [7] would be

$$S = \sqrt{\left\{\int_{-\frac{z_0}{2}}^{\frac{z_0}{2}} M \cos(az^2 + P_{sus}z)\, dz\right\}^2 + \left\{\int_{-\frac{z_0}{2}}^{\frac{z_0}{2}} M \sin(az^2 + P_{sus}z)\, dz\right\}^2} \qquad [12]$$

Note that the imaginary part (Eq. [11]) is no longer zero. Eqs. [8] and [12] are calculated numerically as a function of the phase gradient (P_{sus}) and the results are shown in Fig. 3 (a) and (b). Fig. 3 (a) represents the signal intensity as a function of the linear phase gradient (P_{sus}) in a voxel where inhomogeneity (linear phase $P_{sus}z$) due to susceptibility exists, and when a conventional slice selection RF pulse is used, i.e., when the field inhomogeneity is the same as that in Fig. 2 (b). In this case, the signal intensity is severely reduced as the the strength of the field inhomogeneity increases. When the quadratic phase RF pulse is applied, however, the total phase distribution in the voxel is modified as seen in Fig. 2 (d) and the corresponding greater signal intensity seen in Fig 3 (b).

The implications of Eqs. [8] and [12], together with Fig. 3 (a) and (b), clearly indicate that a quadratic phase RF pulse can greatly enhance the total signal intensity, given the linear field gradient due to susceptibilitys such as that shown in Fig. 2 (b). Moreover, the uniform region of the signal graph in Fig. 3 (b) indicates that the signal strength is quite independent from the strength of the susceptibility. Note also that the signal strength would be reduced to $MZ_o/2$ but the signal strength remains quite constant up to a relatively high field inhomogeneity.

III. Experimental Results and Conclusions

Based on the theoretical discussions above, experiments have been performed using the KAIS 2.0 T whole-body NMR system. To demonstrate that the usage of the tailored RF pulse leads to a reduction of signal loss due to susceptibility, human imagings have been performed with the gradient echo sequence. The repetition time was 500 msec with the echo time of 15 msec and the slice thickness was 1 cm. To reduce the susceptibility effect, the RF pulse was designed so that it results in a quadratic phase distribution in the selected slice. Using the tailored RF pulse shown in Fig. 4 (c), the calculated magnitude and phase distributions were obtained by numerical computation of the Bloch equation and RK4 method (19). The results are shown in Fig. 4 (d). To compare the results obtained with the conventional RF pulse, the same numerical calculation was performed with the RF pulse shown in Fig. 4 (a), and the resulting magnitude and phase distributions are also shown in Fig. 4 (b). Note that the phase distribution within the selected slice using the conventional RF pulse is nearly constant. With the tailored RF pulse, in addition to the phase distribution, the required peak amplitude is much smaller than the conventional pulse; thus much less power is required. Only about 70 % of the normal power is required with the tailored RF pulse.

Finally, a human head imaging near the nasal cavities was performed with and without quadratic phase RF pulse. The image shown in Fig. 5 (a) was obtained using the conventional RF pulse (without a quadratic phase) for the area around the nasal cavities. As is seen, a strong susceptibility artifact is exhibited near the nasal cavities. Fig. 5 (b) is the image obtained applying the quadratic phase RF pulse. In this latter image, the susceptibility artifact is significantly reduced and it shows that all the tissue previously lost due to the susceptibility-dependent signal voids near the nasal cavities (dark area) is recovered.

In conclusion, the proposed quadratic phase RF pulse

technique is found to be useful in compensating for the inhomogeneity in general, and for strong local inhomogeneity due to susceptibility in particular. The power requirement of the tailored RF pulse, moreover, is much less than that of the conventional RF pulse. The proposed method appears particularly useful in many fast gradient echo imaging techniques where image artifacts are predominantly caused by susceptibility.

References

1. H. Y. Carr, *Phys. Rev.* **112**, 1693 (1958).
2. R. C. Hawkes, S. Patz, *Magn. Reson. Med.* **4**, 9 (1987).
3. K. Sekihara, *IEEE Trans. Med. Imag.* **6**, 157 (1987).
4. Y. Zur, S. Stokar, P. Bendel, *Magn. Reson. Med.* **6**, 175 (1988).
5. A. Hasse, J. Frahm, D. Matthaei, W. Hänicke, K. D. Merboldt, *J. Magn. Reson.* **67**, 258 (1986).
6. J. Frahm, W. Hänicke, K. D. Merboldt, *J. Magn. Reson.* **72**, 307 (1987).
7. H. Weber, D. Purdy, M. Deimling, A. Oppelt, *Abstr. Soc. Magn. Reson. Med.,5th Annual meeting*, 18 (1986).
8. A. Oppelt, R. Graumann, H. Barfuss, H. Fisher, W. Hartl, W. Schajor, *Electromedica* **54**, 15 (1986).
9. K. M. Lüdeke, P. Roschmann, R. Tischler, *Magn. Reson. Imagn.* **3**, 329 (1985).
10. H. W. Park, Y. M. Ro, and Z. H. Cho, *Phy. Med. Biol.* **33**, 339 (1988).
11. I. R. Young, S. Khenia, D. G. T. Thomas, C. H. Davis, D. G. Gadian, I. J. Cox, B. D. Ross, G. M. Bydder, *J. of Comp. Assit. Tomog.*, **11**, 2 (1987).
12. Y. S. Kim, C. W. Mun, Z. H. Cho, *Magn. Reson. Med.* **4**, 452 (1987).
13. Y. M. Ro, W. S. Kim, M. H. Cho, Z. H. Cho, To be presented in SMRM, New York, Aug., 1990.
14. I. R. Young, I. J. Cox, D. J. Bryant, G. M. Bydder, *Magn. Reson. Imag.* **6**, 585 (1988).
15. J. Frahm, K. D. Merboldt, W. Hänicke, *Magn. Reson. Med.* **6**, 474 (1988).
16. S. Patz, S. T. S. Wong, M. S. Roos, *Magn. Reson. Med.* **10**, 194 (1989).
17. D. Kunz, *Magn. Reson. Med.* **3**, 377 (1986).
18. S. Conolly, D. Nishimura, A. Marcovski, *J. Magn. Reson.* **78**, 440 (1988).
19. M. J. Maron, "Numerical Analysis", Chap. 8, Macmillian Inc., 1982

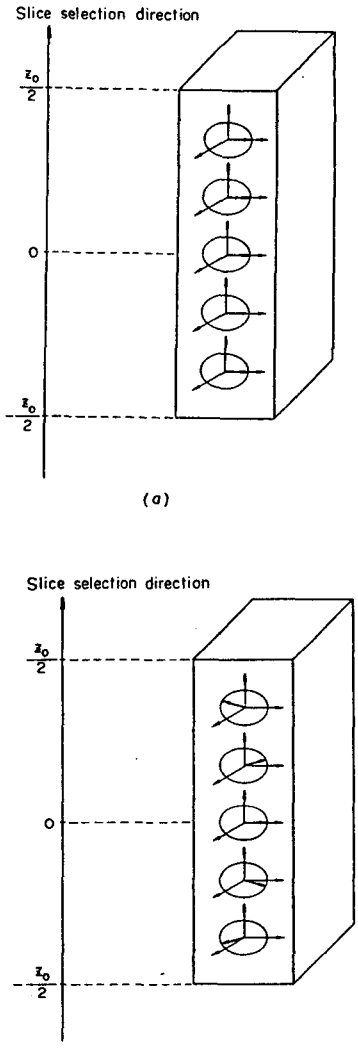

Figure 1 : The simplified illustrations of the spin phase distributions in a voxel.
(a) Spins flip on the transverse plane after the excitation of a RF pulse. They remain in the same phase after echo time (TE) when the fields are homogeneous.
(b) Spins are dephased after echo time (TE) when field inhomogeneity exists.

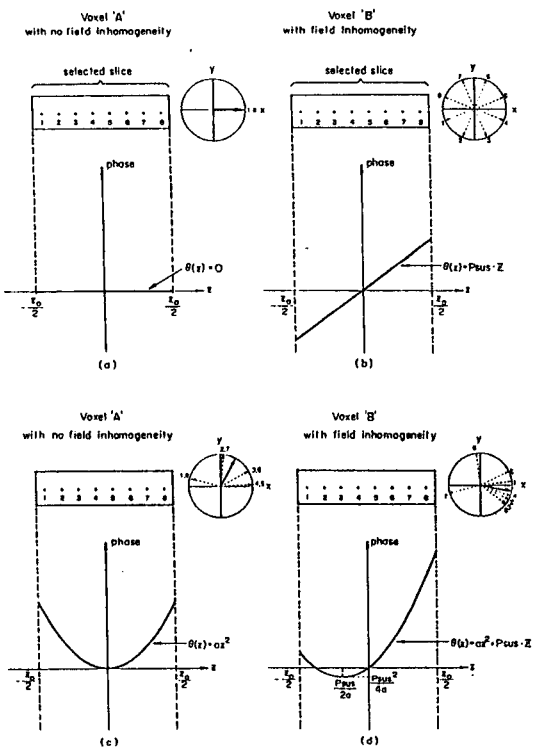

Figure 2 : (a) The phase distribution of the spins in the voxel will be constant when the field is homogeneous.
(b) The phase distribution of the spins in the voxel when a strong localized field gradient exists (e.g. susceptibility).
(c) The phase distribution of the spins in the voxel when a quadratic phase RF pulse is added onto a voxel with a homogeneous field.
(d) The phase distribution of the spins in the voxel when the quadratic phase RF pulse is superimposed on a voxel with the linear field gradient (inhomogeneity) created by the susceptibility.

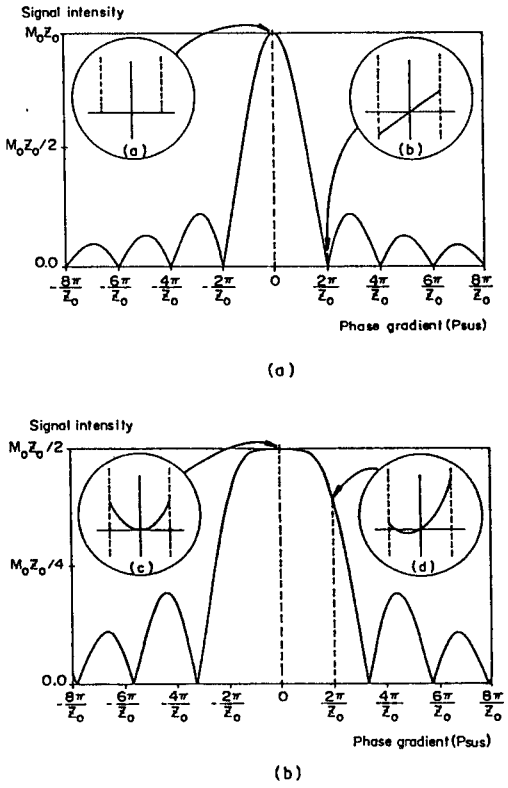

Figure 3 : (a) Signal intensity distribution in the voxel as a function of the strength of the field inhomogeneity (see Fig. 2 (b)).
(b) Same as (a) but with the superimposition of the quadratic phase RF pulse on field inhomogeneity shown in Fig. 2 (b). As seen, the signal intensity as a function of the strength of the field inhomogeneity (susceptibility) is improved substantially in comparison with (a).

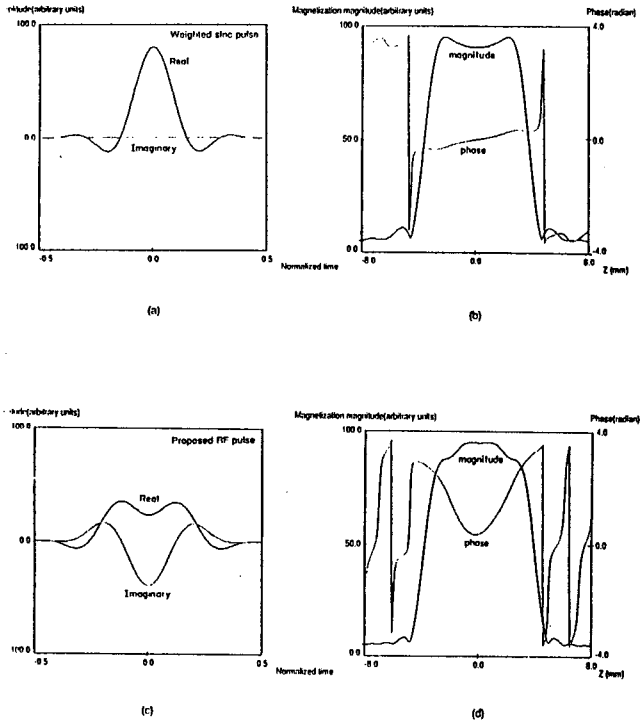

Figure 4 : (a) The real and imaginary parts of the conventional RF pulse.
(b) The magnitude and its phase distribution obtained with the conventional RF pulse shown in (a). This is figured by numerically calculating the Bloch equation with the RK4 method. Note that there is very little phase variation within the selected slice.
(c) The real and imaginary parts of the RF pulse designed to provide quadratic phase distribution in the selected slice.
(d) The same numerical calculation of the magnitude and phase distributions in the selected slice obtained by using the tailored RF pulse shown in (c). As seen, the phase distribution follows a quadratic pattern within the selected slice.

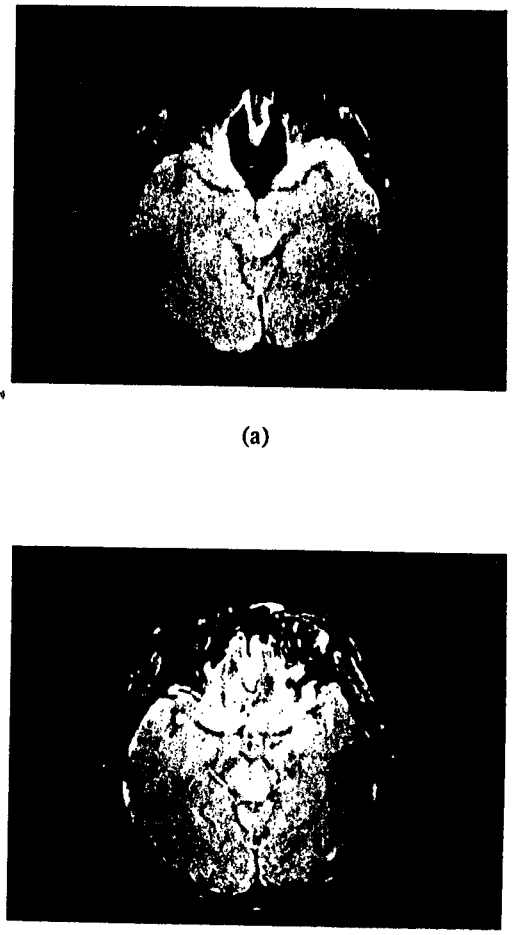

Figure 5 : (a) A human head image obtained with the conventional gradient echo technique. Note the signal void around the nasal cavities.
(b) Same image as (a) obtained with the proposed quadratic phase RF pulse. Note the complete recovery of the signals near the nasal cavities.